# Imaged based analysis of pulmonary arterial network

M. U. Qureshi[1], P. Lee[2], B. E. Carlson[2], T. Sochi[3], N. P. Smith[3], N. Chesler[4], I. Koghan[1], D. A. Beard[2], M. S. Olufsen[1]

[1]Department of Mathematics, North Carolina State University, [2]Department of Molecular & Integrative Physiology, University of Michigan

[3]Imaging Sciences & Biomedical Engineering Division, King's College London, [4]Department of Biomedical Engineering, University of Wisconsin at Madison

The Virtual Physiological Rat Project

## Overview

Understanding the structural changes in pulmonary arterial network with pressure may provide an insight into the structure – function relation and improve our understanding about the genesis of cardiovascular disease such as the pulmonary hypertension. In this study we are aimed to analyze the data obtained from micro-computed tomography images of an excised normotensive mouse lung perfused at four different pressures. Some preliminary results show the variations in the branching patterns, scaling ratios between parent and daughter vessels and averaged length to radius relations across different generations within each structure. However, all the analysis is subject to experimental uncertainties and propagated errors due to image segmentation and reconstruction. Quantifying these uncertainties is the next big goal.

## Methods

① **Imaging:** Mouse lungs for micro-computed tomography was prepared as described in Vanderpool et al. (2011). Briefly, the isolated lung was rinsed free of blood, ventilated with room air and perfused with perfluorooctyl bromide (PFOB). The the lung was placed in the imaging chamber and rotated in the X-ray beam at 1° increments to obtain 360 planar images to complete computed tomography scans by setting the pressure to 7.4, 6.3, 13.0 and 17.2 mmHg respectively. A schematic of the imaging system and original images of arterial vasculature from the micro-Ct are shown in Figure 1.

② **Reconstruction:** Computational reconstruction from the micro-CT images was performed using the approach detailed in Goyal et al. (2013). Briefly the vascular tree was reconstructed as a 3D model of spline-fitted centerlines and associated radii by first enhancing the vessels in the raw CT and then by binarizing and thinning to define the centerlines of all the vessel segments in the segmented vasculature. A model-based method was used to measure radii of each of the vessel segments.

③ **Data Analysis:** The network at each pressure $P_i$ ($i$ = 1,...,4) is represented by two sets, containing real matrices of centerline coordinates and the radii for each vessel within the network

$$V(P_i)=\{[\mathbf{v}_k]_{n\times 3}\} \text{ and } \text{rad}(P_i)=\{[\mathbf{r}_k]_{1\times n}\} \text{ where } k=1,...K_i,\ \ n=1,...N_k.$$

Here $K$ is population size of the network at each pressure and $N$ is the number of landmarks or measuring locations along each vessel. In order to determine connectivity and analyze the branching properties of the network another set, $E(P_i)$, of 2x3 matrices can be extracted from $V(P_i)$ to define the top and bottom nodes of each vessel as the first and last point on the centerline of each vessel. From this point on we view the vascular network as a **directed graph G(E,V)** and use the following analogies

- E(G): Set of vertices (Nodes) V(G): Set of directed edges (vessels)
- Nodes: A point in space where a vessel begins or ends.
- Vessel: A direct edge between two nodes
- Indegree of E: number of vessels ending at E
- Outdegree of E: number of vessels starting at E

**Theorem:** Sum(outdegree(E(G)) = Sum(indegree(E(G)) = cardinality(V(G))

- Junctions: A node E such that indegree(E) ≠ 0 and outdegree(E) ≠ 0.
  **Examples**: Bifurcation, Trifurcation, Quadfurcation, Monode.
- Root: A Node R with indegree(R) = 0 and oudegree(R) = 1. Associated vessel is the root vessel
- Terminals: A node T with indegree(T) ≠ 0 and outdegree(T) = 0. Associated vessels are the terminal vessels
- Loops: If indegree(node) > 1. Generation: Number of junctions between a given vessel and the root vessel

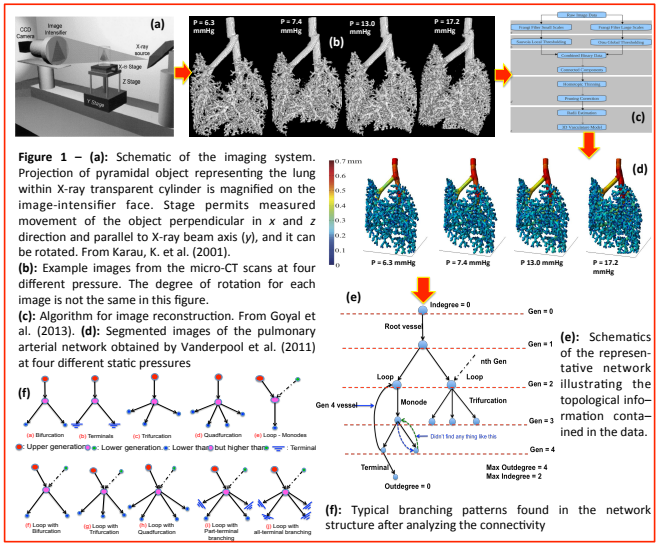


**Figure 1 – (a):** Schematic of the imaging system. Projection of pyramidal object representing the lung within X-ray transparent cylinder is magnified on the image-intensifier face. Stage permits measured movement of the object perpendicular in $x$ and $z$ direction and parallel to X-ray beam axis ($y$), and it can be rotated. From Karau, K. et al. (2001). **(b):** Example images from the micro-CT scans at four different pressure. The degree of rotation for each image is not the same in this figure. **(c):** Algorithm for image reconstruction. From Goyal et al. (2013). **(d):** Segmented images of the pulmonary arterial network obtained by Vanderpool et al. (2011) at four different static pressures **(e):** Schematics of the representative network illustrating the topological information contained in the data. **(f):** Typical branching patterns found in the network structure after analyzing the connectivity

## Structure Analysis

**Length and Radius:** $\forall \mathbf{v}_k \in V(P_i),\ L(\mathbf{v}_k)=\sum_{j=1}^{N_k-1}\left\|X_{j+1}(x,y,z)-X_j(x,y,z)\right\|,\ r(\mathbf{v}_k)=\frac{1}{N_k}\sum \mathbf{r}_k$

**Scaling Factors:** $\alpha=r_{d1}/r_p,\ \ \beta=r_{d2}/r_p$ **Area Ratio:** $\eta=\frac{r_{d1}^2+r_{d2}^2}{r_p^2}=\alpha^2+\beta^2$

**Asymmetry Ratio:** $\gamma=r_{d2}/r_{d1}=\beta/\alpha$ **Length to Radius Ratio:** $L_{rr}=\frac{L(\mathbf{v}_k)}{r(\mathbf{v}_k)}$

## Tree Resistance

- **Resistance of a single vessel:** $R=\frac{128\mu(D)L}{\pi D^4}$ where $D=2r$ is in $\mu$m.
- **Resistance at a given generation:** $R_{\|}(gen)=\frac{1}{\frac{1}{R_1}+\frac{1}{R_2}+...+\frac{1}{R_n}}$
- **Total Resistance:** $R_T(V)=\sum_{gen=1}^{n} R_{\|}(gen)$

## Data Statistics

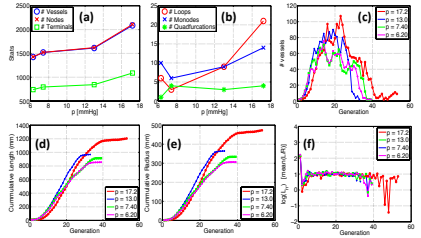


**Figure 2 (a) & (b):** Variations in the network population and branching patterns. **(c):** Variations in the population with pressure at each generation. **(d) & (e):** Pressure induced changes in the cumulative network radius and path length. **(f):** Length to radius relation across network generations at different pressure

| P (mmHg) | Radius (mm-micron) | Length (mm-micron) | Cumulative Network Length (mm) | Cumulative Network Radius (mm) | Number of Generations | Network Resistance using mean radius | Network Resistance using median radius |
|---|---|---|---|---|---|---|---|
| 6.3 | 0.6 – 96 | 5.002 – 40 | 855 | 306 | 39 | 4346 | 3342 |
| 7.4 | 0.612 – 121 | 5.0710 – 57 | 914 | 334 | 39 | 6393 | 3607 |
| 13.0 | 0.634 – 89 | 5.178 – 40 | 969 | 364 | 33 | 1126 | 744 |
| 17.2 | 0.681 – 79 | 5.359 – 40 | 1204 | 473 | 53 | 484.4 | 310 |

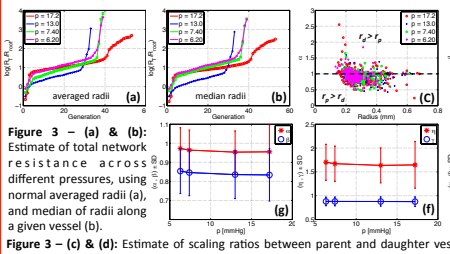


**Figure 3 – (a) & (b):** Estimate of total network resistance across different pressures, using normal averaged radii (a), and median of radii along a given vessel (b).

**Figure 3 – (c) & (d):** Estimate of scaling ratios between parent and daughter vessels across all bifurcating junctions as a function of radius. **(e):** Scaling ratios distributed and averaged over bins of radius range found for P = 17.2 mmHg. **(f) & (g):** Variations in network averaged scaling ratios, area ratios and asymmetry ratios for all the bifurcating junction with pressure.

## Discussion

In this study, we have presented some preliminary results to analyze the structure of a mouse pulmonary arterial vasculature across different pressures. We observe some unexpected branching patterns including loops in the flow paths and generation of a thicker daughter vessel from a thinner parent vessel. Also, we expect the network resistance to go down as a result of increase in total cross-section area due to pressure. However, for p = 7.4 mmHg, the resistance is greater than when p = 6.3 mmHg, using normal mean to estimate the vessel radius. This improves slightly when median is used as a measure of average radius.

## References

1. Vanderpool, Rebecca R. et al. (2011) *J Appl Physiol*, 110:188-198
2. Karau, K. et al. (2001) *Am J Physiol Heart Circ Physiol*, 281: 2747 – 2756
3. Goyal, A. et al. (2013) *IEEE Trans Med Imaging*, 32(1):56 – 72

## Acknowledgements

Funding for this research is provided by the virtual physiological rat center via NIH-NIGMS grant #1P50GM094503-01A0